

# Optical Emission Spectroscopy Diagnostics of Electron Density and Temperature for Atmospheric-Pressure Helium Plasma Based on a Collisional-Radiative Model

K. Lin<sup>1</sup>, A. Nezu<sup>2</sup> and H. Akatsuka<sup>3</sup>

<sup>1</sup> Department of Electronic and Electrical Engineering, Tokyo Institute of Technology, Tokyo, Japan

<sup>2</sup> Open Facility Center, Tokyo Institute of Technology, Tokyo, Japan

<sup>3</sup> Institute of Innovative Research, Tokyo Institute of Technology, Tokyo, Japan

**Abstract:** The conventional helium collisional-radiative (CR) model is updated by including atomic collision processes. An algorithm is developed to determine the electron density and temperature of atmospheric pressure helium plasma based on the revised CR model. It fits eight emission lines (3<sup>1</sup>S, 3<sup>3</sup>S, 3<sup>1</sup>P, 3<sup>3</sup>P, 3<sup>1</sup>D, 3<sup>3</sup>D, 4<sup>1</sup>D, and 4<sup>3</sup>D) in the visible-wavelength range by the electron density, electron temperature, ground state density, and the populations of two metastable levels (3<sup>1</sup>S and 3<sup>3</sup>S). Electron density and temperature diagnosed by the algorithm agree well with the results measured with probe method at low-pressure. Results of the algorithm are also in good agreements with results of the continuum spectrum analysis at atmospheric pressure.

**Keywords:** Helium, collisional-radiative model, optical emission spectroscopy.

## 1. Introduction

Optical emission spectroscopy (OES) is widely used for diagnosing plasma parameters of various types of plasma. The continuum spectrum analysis based on atmospheric pressure argon CR model has been developed for determining the electron density and temperature of argon plasma [1-2]. OES diagnosis of low-pressure helium based on helium CR model has also been researched in many studies [3-5]. However, there is no effective method to determine the electron density and temperature of atmospheric pressure helium plasma.

In this study, the development of an atmospheric-pressure helium CR model is demonstrated. An algorithm for diagnosing the electron density and temperature as well as the number density of two metastable states by fitting the results of OES measurements has been developed based on the new model.

## 2. Methodology

Firstly, we should make sure the CR model available at atmospheric pressure. Atomic collision processes are included to the conventional helium CR model. Figure 1 schematically shows the processes considered in the new model.

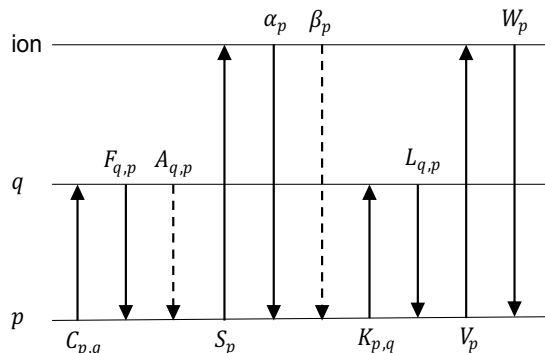


Fig. 1. Population and depopulation processes in the atmospheric pressure helium CR model. The solid and dashed lines represent collisional and radiative processes, respectively.

$C_{p,q}$  and  $F_{p,q}$  are the rate coefficients of electron collision excitation and de-excitation, respectively.  $A_{p,q}$  is the Einstein's A coefficient, while  $S_p$  is the electron collision ionisation rate coefficient.  $\alpha_p$  and  $\beta_p$  are the electron three-body and radiative recombination rate coefficients, respectively.  $K_{p,q}$  and  $L_{p,q}$  are the rate coefficients of atom collision excitation and de-excitation, respectively.  $V_p$  and  $W_p$  are the atomic collision ionisation and atomic three-body recombination rate coefficients, respectively.  $p$  and  $q$  represent the ground state 1<sup>1</sup>S ( $p$  or  $q = 1$ ) or any excited state ( $p$  or  $q = 2, 3, 4, \dots, 65$ ) that are different from each other. The temporal development of the number density of level  $p$  at atmospheric pressure can be described as

$$\begin{aligned} \frac{dN_p}{dt} = & \sum_{q < p} C_{q,p} N_e N_q + \sum_{q > p} F_{q,p} N_e N_q + \\ & \sum_{q > p} A_{q,p} N_q - \sum_{q > p} C_{p,q} N_e N_p - \sum_{q < p} F_{p,q} N_e N_p \\ & - \sum_{q < p} A_{p,q} N_p - S_p N_e N_p + \alpha_p N_e^2 N_i + \\ & \beta_p N_e N_i - \sum_{q < p} K_{q,p} N_1 N_q + \sum_{q > p} L_{q,p} N_1 N_q - \\ & \sum_{q < p} L_{p,q} N_1 N_p - V_p N_1 N_p + W_p N_1 N_e N_i. \end{aligned} \quad (1)$$

Except the ground state and two metastable states, the time derivative on the left-hand-side of eq. (1) can be neglected:

$$\frac{dN_p}{dt} = 0 \quad (p \geq 4). \quad (2)$$

Then, the rate equation of these levels can be written as

$$\begin{pmatrix} \zeta_{1,4} & \zeta_{2,4} & \zeta_{3,4} & -\zeta_4 & \zeta_{5,4} & \zeta_{6,4} & \dots & \zeta_{65,4} \\ \zeta_{1,5} & \zeta_{2,5} & \zeta_{3,5} & \zeta_{4,5} & -\zeta_5 & \zeta_{6,5} & \dots & \zeta_{65,5} \\ \zeta_{1,6} & \zeta_{2,6} & \zeta_{3,6} & \zeta_{4,6} & \zeta_{5,6} & -\zeta_6 & \dots & \zeta_{65,6} \\ \vdots & \vdots & \vdots & \vdots & \vdots & \vdots & \ddots & \vdots \\ \zeta_{1,65} & \zeta_{2,65} & \zeta_{3,65} & \zeta_{4,65} & \zeta_{5,65} & \zeta_{6,65} & \dots & -\zeta_{65} \end{pmatrix}$$

$$\times \begin{pmatrix} N_1 \\ N_2 \\ N_3 \\ N_4 \\ N_5 \\ N_6 \\ \vdots \\ N_{65} \end{pmatrix} = \begin{pmatrix} -\zeta_{ion,4} \\ -\zeta_{ion,5} \\ \vdots \\ -\zeta_{ion,65} \end{pmatrix} N_1 \quad (3.a)$$

with

$$\zeta_{q,p} = C_{q,p}N_e + A_{q,p} + K_{q,p}N_1, \quad (3.b)$$

$$\zeta_p = S_pN_e + V_pN_1 \sum_{p \neq q} (C_{p,q}N_e + A_{p,q} + K_{p,q}N_1), \quad (3.c)$$

and

$$\zeta_{ion,p} = -\alpha_p N_e N_1 - \beta_p N_e - W_p N_e N_1. \quad (3.d)$$

It should be noted that to simplify the expression,  $C_{p,q}$ ,  $F_{p,q}$  and  $K_{p,q}$ ,  $L_{p,q}$  are written as single rate coefficients.  $F_{p,q}$  is replaced by  $C_{p,q}$ , and  $L_{p,q}$  is replaced by  $K_{p,q}$  when  $p > q$ . Since all rate coefficients can be calculated after temperature is known [6-11], the populations of all levels  $p$  ( $p \geq 4$ ) can be solved if  $N_e$ ,  $T_e$ ,  $T_g$ ,  $N_1$ ,  $N_2$ , and  $N_3$  is input.

To determine electron density and temperature based on number density of eight levels ( $3^3P$ ,  $4^3D$ ,  $4^1D$ ,  $3^1P$ ,  $3^3D$ ,  $3^1D$ ,  $3^3S$ , and  $3^1S$ ), an algorithm was developed to inversely solve the model. Genetic algorithm [12] is applied to optimize the object function in the algorithm:

$$f_{obj} = \sum_{p=6,7,8,9,10} \left( \frac{N_p^{exp} - N_p^{cal}}{N_p^{small}} \right)^2, \quad (4)$$

where  $N_p^{exp}$  and  $N_p^{cal}$  are the number density of level  $p$  measured in experiment and counterpart calculated by the algorithm.  $N_p^{small}$  equals to the smaller between  $N_p^{exp}$  and  $N_p^{cal}$ .

### 3. Results and Discussion

Electron density and temperature of microwave induced low-pressure helium plasma determined by the algorithm

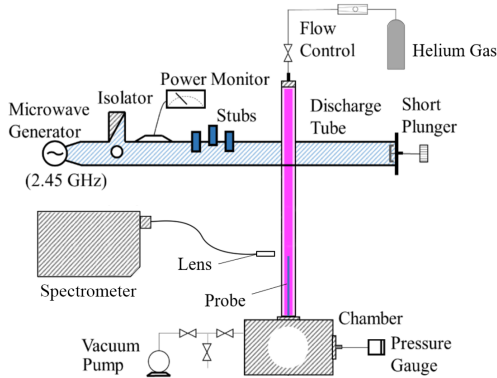


Fig. 2. Layout of the low-pressure microwave helium discharge system. The measurement position  $z$  is the distance from the centre of the wave guide to the position where the plasma is measured.

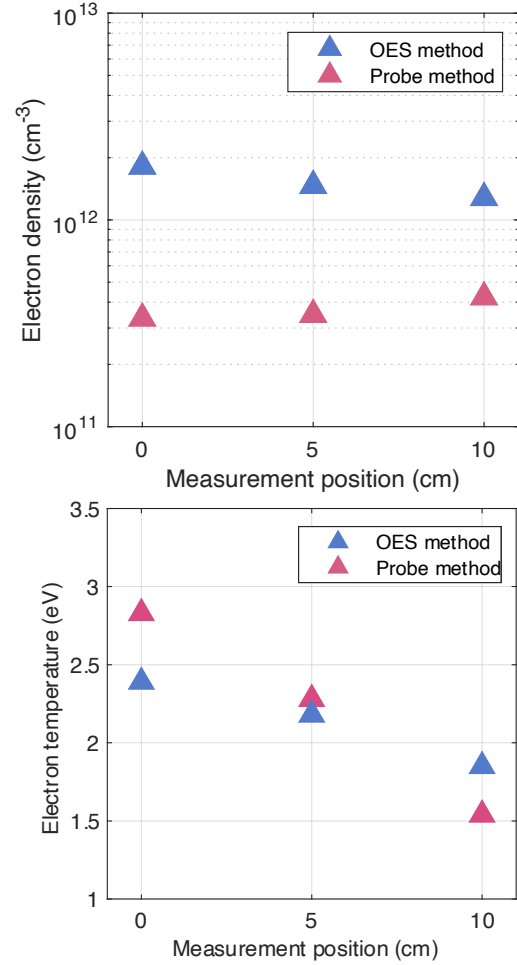


Fig. 3. Comparison of results between OES diagnosis and probe method. (a) Determined electron density, (b) Determined electron temperature.

were compared with those obtained by the probe method. The structure of the discharge system is shown in Fig. 2.

The results measured in different measurement position  $z$  at 1 Torr are shown in Fig. 3. The electron density determined by the two methods is of the same order of magnitude, and the measured electron temperature is similar. Thus, it can be assumed that the results of the algorithm at low pressure,  $P = 1$  Torr agree well with those of the probe method.

The algorithm is also used for diagnosing the non-equilibrium atmospheric-pressure helium plasma as shown in Fig. 4.

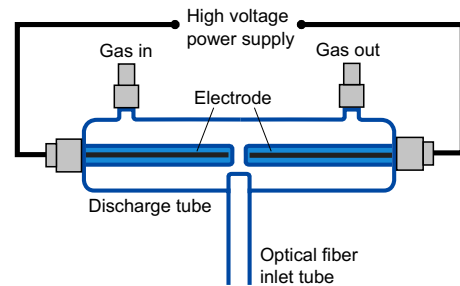


Fig. 4. Schematic overview of the atmospheric-pressure non-equilibrium discharge plasma generator.

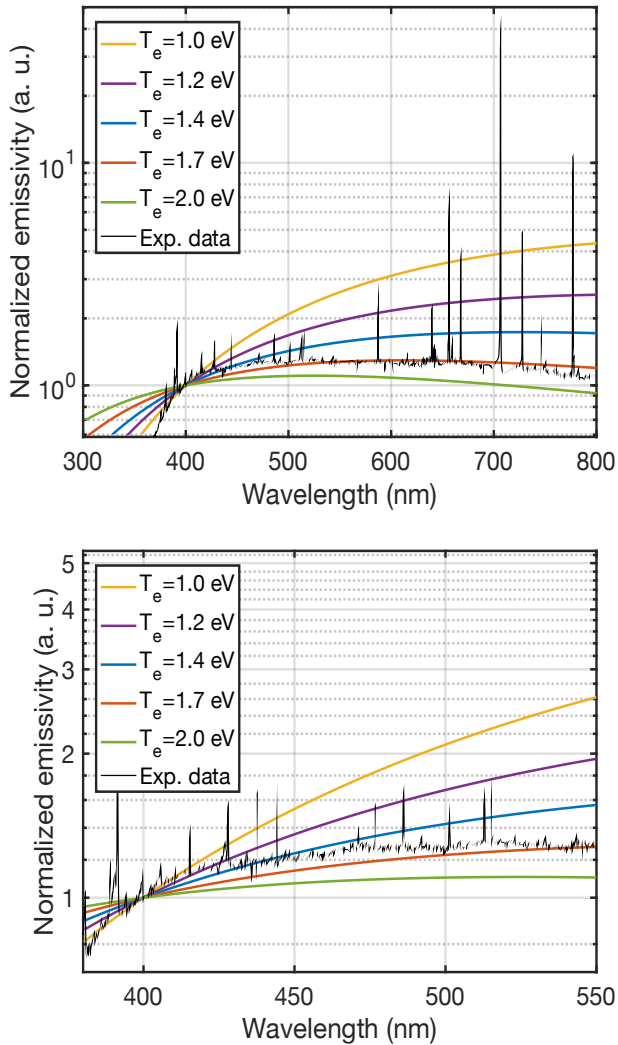


Fig. 5. Fitting of the emission spectrum of the atmospheric-pressure plasma in the visible range by the normalized emissivity with Eq. (31). (a) Normalized emissivity in the range of 300-800 nm. (b) Normalized emissivity in the range of 380-550 nm.

The comparison between the results of the algorithm and the continuum spectrum analysis is shown in Fig. 5. Figure 5 (a) shows that an electron temperature of 1.7 eV, the theoretical emissivity was best agreed with the experimental data. The theoretical value was slightly lower than the emissivity measured in the experiment from 400 to 550 nm and exceeded the experimental data from 700 to 800 nm. Figure 5 (b) indicates that the blue line ( $T_e = 1.4$  eV) has a relatively better fit with the experimental data in the range of 400 – 470 nm. In general, the electron density and temperature obtained by the algorithm in this study were  $3.2 \times 10^{10} \text{ cm}^{-3}$  and 1.42 eV, respectively. Those obtained by the continuum spectrum analysis were  $2.6 \times 10^{10} \text{ cm}^{-3}$  and 1.7 eV, respectively. It can be considered that the results of the algorithm agree well with the results of the continuum spectrum analysis in atmospheric pressure non-equilibrium helium plasma experiment.

#### 4. Conclusion

In this study, the valid pressure of the conventional CR model was extended to atmospheric pressure by including atomic collision processes. The developed algorithm is able to diagnose the electron density and temperature by inputting number density of eight states ( $3^3\text{P}$ ,  $4^3\text{D}$ ,  $4^1\text{D}$ ,  $3^1\text{P}$ ,  $3^3\text{D}$ ,  $3^1\text{D}$ ,  $3^3\text{S}$ , and  $3^1\text{S}$ ) that can be measured in the visible wavelength range using the OES method. The results in the low-pressure and atmospheric pressure experiment showed the electron density and temperature determined by the algorithm were reasonable.

#### 5. References

- [1] H. Onishi, F. Yamazaki, Y. Hakozaiki, M. Takemura, A. Nezu, and H. Akatsuka, *Jpn. J. Appl. Phys.* **60**, 026002 (2021).
- [2] H. Akatsuka, *Phys. Plasmas* **16**, 043502 (2009).
- [3] M. Goto and K. Sawada, *J. Quant. Spectrosc. Radiat. Transfer* **137**, 23 (2014).
- [4] M. Goto, *J. Quant. Spectrosc. Radiat. Transfer* **76**, 331 (2003).
- [5] K. Lin, A. Nezu, and H. Akatsuka, *Jpn. J. Appl. Phys.* **61**, 116001 (2022)
- [6] Yu. V. Ralchnko, R. K. Janev, T. Kato, D. V. Fursa, I. Bray, and F. J. de Heer, Cross Section Database for Collisional Processes of Helium Atom with Charged Particles. I. Electron Impact Processes, Rep. NIFS-DATA-59, NISF, Nagoya, Japan (2000).
- [7] M. B. Shah, D. S. Elliott, P. McCallion, and H. B. Gilbody, *J. Phys. B.* **21**, 2751 (1988).
- [8] T. Fujimoto, Semi-empirical Cross Section and Rate Coefficients for Excitation and Ionization by Electron Collision and photoionization of Helium, Rep. IPP-AM-8, (Institute of Nagoya Physics, Nagoya University, Nagoya, Japan, 1978).
- [9] M. Goto and T. Fujimoto, Collisional-radiative Model for Neutral Helium in Plasma: Excitation Cross Section and Singlet-triplet Wave-function Mixing, Rep. NIFS-DATA-43, NISF, Nagoya, Japan (1997).
- [10] G. Gousset and C. Boulmer-Leborgne, *Journal de Physique* **45** (4), 689 (1984).
- [11] L. C. Cusachs and H. S. Aldrich, *Chem. Phys. Lett.* **12** (1), 197 (1971).
- [12] S. Sivanandam, and S. Deepa, “Genetic Algorithm Implementation Using Matlab”. *Introduction to Genetic Algorithms*, Springer, Berlin, Heidelberg (2008).